

Experimental and Numerical Investigation on Aerodynamic Characteristics of Darrieus Rotor Using Directed Guide Vane

First Student Author: Helmy Y. Helmy*

Mechanical Power Engineering Dept., Higher Technological Institute 10th of Ramadan City, Egypt, P.O. Box: 228
Email: 20170303@hti.edu.eg

Supervisor: Radwa A. Ghazala, Assistant professor at Mechanical Power Engineering Dept.,
Higher Technological Institute 10th of Ramadan City, Egypt, Radwa.ghazala@hti.edu.eg

Abstract– Darrieus wind turbines (DWT) are preferable type of Vertical axis wind turbines at domestic zones that characterized by low wind speed, but low performance is obtained compared quantitatively to other categories of wind turbines. The current study introduces the effect of varying the angles of directed guide vanes (DGVs) on the performance of Darrieus rotor. For this purpose, the experiment test is carried out to determine the highest power coefficient. The numerical model is simulated using three different straight-bladed Darrieus rotor via two-dimensional (2D) computational fluid dynamics (CFD). A grid and mesh independency test as well as the effect of domain size, are conducted and a suitable agreement is obtained. The directed guide vane augmented with the rotor is simulated for two angles of the DGV at different five tip speed ratios (TSR), to investigate the impact of guide vanes angles on the VAWT performance. The results of the present study indicated that output power of the VAWT with $a = 20$ and $b = 55$ DGV guide vanes, was improved 16.9%, 38.8%, 42.2%, 27.4% and 27.7%, respectively in four different TSR including 3, 4, 5, 6 and 7.

Keywords– Darrieus rotor, directed guide vane, CFD, Turbulence model, aerodynamic

1. INTRODUCTION

The demand on energy is creeping up every day due to rapid growth of population, industrial and agricultural. The fossil energy sources are becoming limited which is ultimately making them more expensive. In addition to this, everyone is concerned about global climate change. The whole scenarios are pushing the world towards the dependency on alternative sources of energy. Wind energy is the most promising source among the other sources of renewable energy. Wind energy has the potential to resolve the power demand of the entire world if it can be converted into electricity efficiently. Wind energy is harvested using two categories of modern wind turbines classified according to their axis of rotation namely, Horizontal Axis Wind Turbine (HAWT) and Vertical Axis Wind Turbine (VAWT). The most famous types of VAWTs are:

- Savonius type (drag type) invented by Finnish engineer S.J. Savonius in 1922. The rotation speed of Savonius wind turbine is lower than wind speed; therefore, it has Tip Speed Ratio (TSR) of 1 or below.
- Darrieus type (lift type) is patented firstly in France (1925) and in U.S. (1931) by Georges Jean-Marie Darrieus. There are two types for Darrieus VAWTs, namely Eggbeater Darrieus rotor and H-Darrieus (H-rotor) as shown in Fig.1. Darrieus wind turbine can rotate in higher speeds than wind speeds so the TSR is greater than 1, but it generates less torque compared to Savonius.

In the last decade VAWTs take more attention from the researchers as it works well in domestic areas. The turbine blades are oriented in Omnidirectional that is suitable for domestic region where the wind direction is frequently changing among the year. VAWTs are suitable for electricity generation due to its quiet behaviour which is more suitable for highly populated places. The cost of complex structure of HAWT blades that should be twisted and tapered for optimum performance is higher than the simpler VAWT blades. The stalling behaviour it can withstand gust wind, which makes it much safer during those weather conditions. VAWT is an appropriate turbine that can be installed in densely populated urban area, away from the main distribution lines and places where large wind farms cannot be installed due to environmental concerns. The main drawbacks of Darrieus turbine are its low performance at built and domestic areas. Therefore, many researchers tried to characterize the most convenient principles of operation to improve the performance of Darrieus turbines, through both experiments and numerical computational methods.

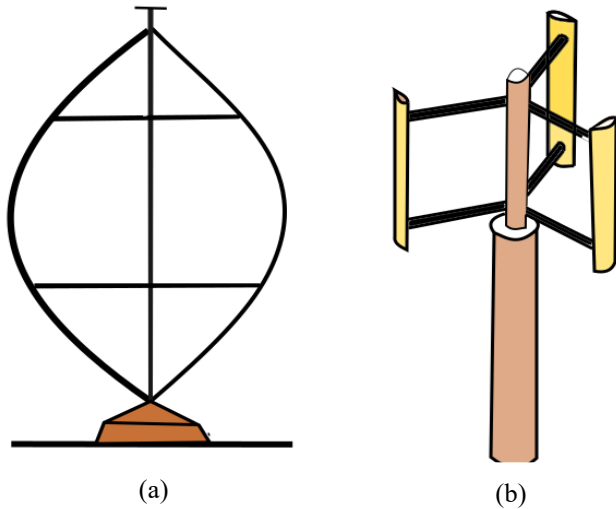


Fig. 1: (a) Egg beater (b) Three-bladed H-rotor

Howell et al. [1] experimented on small scale Darrieus rotor. The experimental study in wind tunnel and computational study is done to find the aerodynamics and performance by changing wind velocity, tip-speed ratio, solidity, and rotor blade surface finish. It is concluded that, below a critical wind speed (Reynolds number of 30,000) a smooth rotor surface finish degraded the performance of the turbine. The tests also showed that both two and three bladed rotor models had produced highest performance coefficient, but the three bladed models are more efficient at a much-reduced Tip Speed Ratio. Beri and Yao [2] studied the effect of camber air foil for a self-starting Darrieus turbine. They tested three bladed NACA 2415 camber air foil at different tip speed ratios. The experimental results showed that, camber air foil have the characteristics of self-starting. Castelli et al. [3] presented 2-D numerical model simulations using NACA 0021 three bladed rotors with a constant wind speed of 6 m/s to investigate the aerodynamic performance of a straight-bladed Darrieus turbine. (Wakui, et al. 2005) [4] is used hybrid configuration of Darrieus lift type with Savonius drag-type rotors. The result showed that Savonius rotor inside the Darrieus rotor had fine operating behaviour to wind speed changes and could be compactly designed because of a shorter rotational axis. This is an effective way for stand-alone small-scale systems. Chong et al. [5] introduced an idea named direction-guide-vane (DGV) to enhance the performance of the VAWT. The DGV could be deployed even in weak low wind speed and turbulent conditions commonly found in urban areas where conventional VAWT are not suitable. It is also capable to accelerate with on-coming wind to improve its energy output and starting characteristic of the wind turbine. Nobile et al. [6] is conducted a 2D CFD analysis to determine mesh, turbulence, and scale of time step, for an augmented VAWT. The results showed that the C_p and C_m were not dependent on incident wind speed that is considered. In the present research, a 2D CFD study was performed to predict the power output of the

VAWT by varying the DGV angles, and results of the VAWT CFD simulation are compared with experimental data. To select the most accurate DGV angles, all CFD steps were verified via grid and time step independency test and various turbulence models.

2. METHODOLOGY AND CODE VALIDATION

2.1 Turbine main features

The geometrical details in Fig.2 of the three straight bladed Darrieus wind turbine were summarized in Table [1].

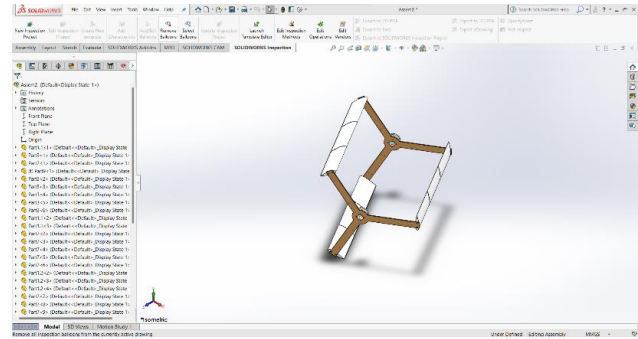


Fig. 2 Schematic diagram of the three straight bladed Darrieus rotor on Solid works

TABLE 1
SPECIFICATION OF DARRIEUS ROTOR

Geometry of turbine	Dimensions
Blade profile	NACA 0021
Blade chord (C)	78 mm
Radius of the turbine (R)	250 mm
Number of the blade (N)	3
Solidity (NC/D)	0.468
Height (H)	500 mm
Aspect ratio (H/D)	1

2.2 DGV main features

The basic design of DGV is fully explained in Table [2] accordingly, the DGV consists of four pairs of guide vanes as illustrated in Fig. 3. The scope of the current study is to compare the C_p for the bare turbine and DGV using 2 different inclination angles for the DGV.

TABLE 2
SPECIFICATION OF DGV

Geometry of turbine	Dimensions
Number of guide vanes	8 (4 pairs)
Inner radius	330 mm
Outer radius	500 mm
Length	120 mm

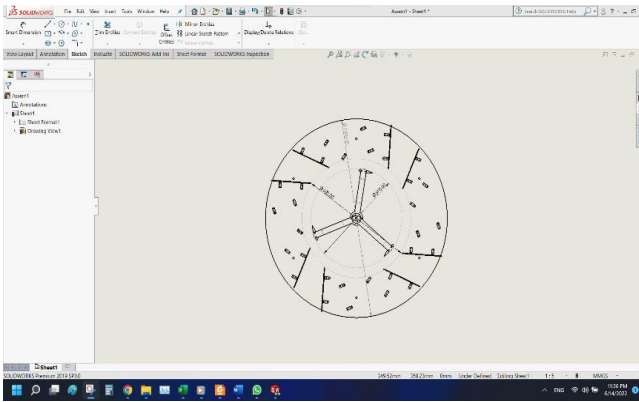
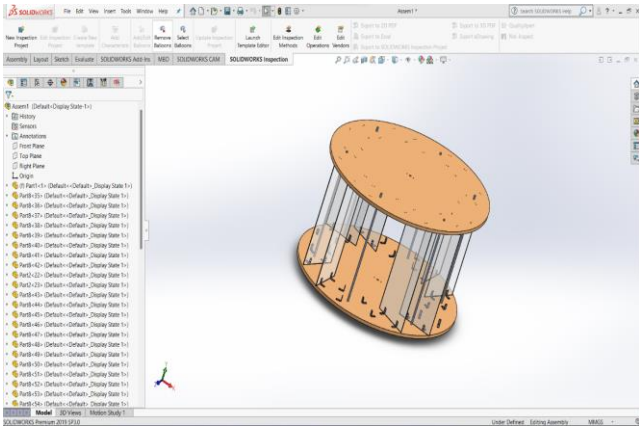


Fig.3 four pairs of DGV

2.3 Domain, mesh, boundary conditions and turbulence model approach

Generating the two-dimensional (2D) VAWT computational domain, meshing, setting the turbulence model and defining its specifications all achieved by using commercial software ANSYS-Fluent. The present numerical model contains two main domains: the rotating inner domain, the stationary domain at the outer and in the middle of the rotating domain. The rotor domain characterized by a moving mesh which has three symmetric air foil blades located on an azimuth angle of 120° relative to each other as shown in Fig.4 with non-slip rotating wall as boundary. A rectangular flow domain with mentioned dimensions is adopted as shown in Fig.5. Unstructured triangular mesh is used for both fixed and rotating grids, to reduce cost time while preparing CFD simulations. The grid transition on each side of the grid interface has nearly the same element size to avoid divergence phenomena of the model and achieving faster convergence. Intensify the meshing using 20 boundary layers with growth rate 1.2 as near as possible from the wall surface of the turbine blades to capture the viscous sub-layer guaranteed that the maximum value of $Y^+ < 1$. Once the grid is generated, the unsteady two-dimensional Navier Stokes equations are solved using a RANS approximation. The boundary conditions are uniform velocity inlet, zero-gauge pressure outlet, symmetry sides and no slip walls (see Table 3). The turbulent length

scale at the domain inlet and outlet is selected based on length scale of the turbine diameter. Pressure-velocity coupling is achieved with the SIMPLE (Semi-Implicit Method for Pressure Linked Equations) algorithm, to allow faster convergences. Gradient in spatial discretization of least squares cell-Based was used to ensure more accurate results. The second order scheme is used for pressure calculations. Second-order discretization is chosen for momentum equations and turbulence equations including turbulent dissipation rate and turbulent kinetic energy equations are discretized using finite volume method with second-order upwind scheme. For time integration, the second order implicit formulation is used.

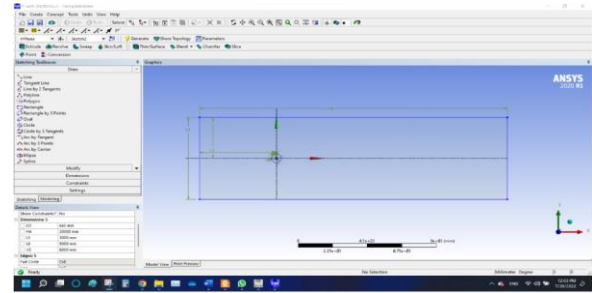


Fig.4 Domain size

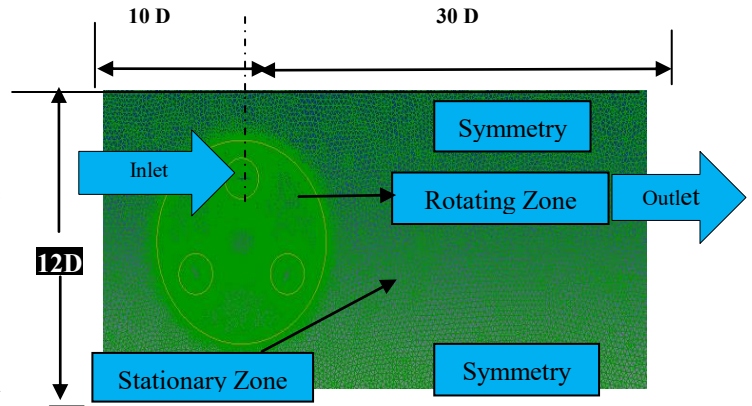


Fig. 5 Boundary condition in domain

TABLE 3
BOUNDARY CONDITION IN DOMAIN

Wall	Boundary condition	
Inlet	Velocity	6 m/s
Outlet	Pressure	0 Pa
Turbine	Wall	No slip walls

On the other hand, the shear stress transport (SST) formulation is formed by combining $k-\omega$ and $k-\epsilon$ models. This structure helps SST method switch to the $k-\epsilon$ model to avoid $k-\omega$ problem in inlet free-stream turbulence properties and uses the $k-\omega$ formulation in the inner parts of the boundary layer. Two mathematical formulas, including k and ω equations, have been proposed in SST methods as below:
Equation k :

$$\text{Equation } k: \frac{\partial}{\partial t}(\rho k) + \frac{\partial}{\partial x_i}(\rho k u_i) = \frac{\partial}{\partial x_j} \left(\Gamma_k \frac{\partial k}{\partial x_j} \right) + G_k - Y_k + S_k \quad (1)$$

$$\text{Equation } \omega: \frac{\partial}{\partial t}(\rho \omega) + \frac{\partial}{\partial x_i}(\rho \omega u_i) = \frac{\partial}{\partial x_j} \left(\Gamma_\omega \frac{\partial \omega}{\partial x_j} \right) + G_\omega - Y_\omega + S_\omega \quad (2)$$

Where, Γ_k and Γ_ω express the active diffusivity of k and ω , as well S_k and S_ω that are user defined source terms. In addition, G_k and G_ω show the turbulence kinetic energy generation due to mean velocity gradients and ω , Y_k and Y_ω also mean the dissipation of k and ω due to turbulence.

2.4 Study of mesh impact on flow field

To study the influence of the mesh on the power output results, grid independency test (GIT) was carried out in this study and three types of mesh were conducted. Fig. 6 shows cut plane of mesh in domain, VAWT, DGV and blade. As can be seen in Fig. 6, around VAWT and specifically around the blades, meshes are highly denser to capture the complex flow structure with lower expected error. As mentioned, the $k-\omega$ SST model was applied as a proper turbulence model in this study. The findings indicated that prediction of CP highly depends on the mesh density especially around the blades and varies less than 20% between 1 and 2 million mesh elements.

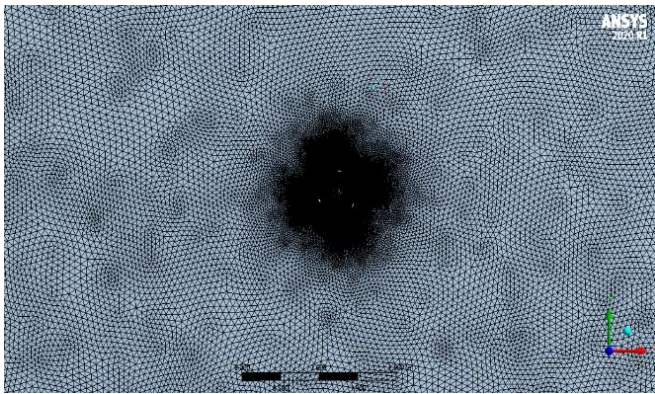


Fig. 6. A

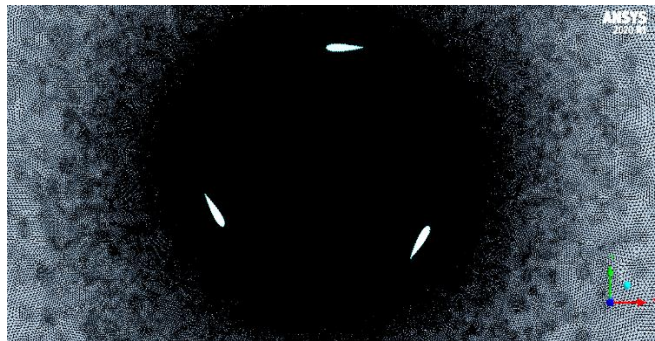


Fig. 6. B

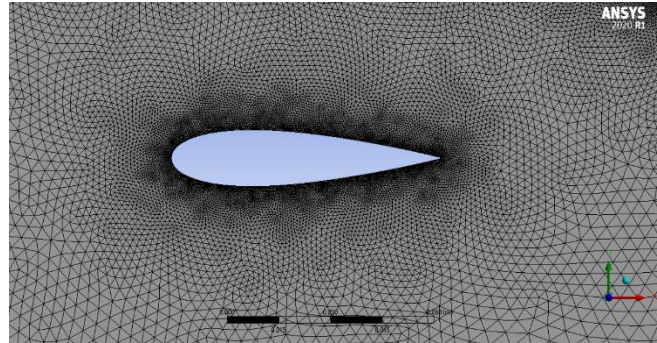


Fig. 6.C
plane of mesh in domain, VAWT, DGV and blade.

3. EXPERIMENTAL TESTING

When we finished manufacturing the turbine and it was manufactured by three steps, the first step is to manufacture the blade using 3D printing, which helps in the manufacture of complex objects easily. The second step is to manufacture the guiding vanes from acrylic using a laser machine, and the third step is to assemble the mechanical parts represented by the shaft, bearing, bushing and flange and the corners of the letter I and screws. Then after manufacturing, the turbine was tested in front of the wind tunnel to simulate the speed and force of the air at a speed of 6 m/s as shown in Fig. 7



Fig. 7 Turbine test using wind tunnel

4. RESULTS AND DISCUSSION

4.1 Influence of the guide vane angle

As mentioned earlier, the most goal of this study is to maximise the output power of VAWT by means of correcting guide vane angles. For this purpose, 2 design points are considered to seek out the simplest guide vanes position and to realize the very best performance of the VAWT. Table 4 shows the position and style points of the various DGV angles.

Table 4
Design points of the different angle of the ODGV.

Design point	β	α
DP1	20	40
DP2	20	55

angles.

In addition, this test was conducted in only four different TSR including 3, 4, 5, 6 and 7 to save time and cost of the simulation, so every design point was simulated for the mentioned four different TSRs. Consequently, 20 simulations have been performed with 7 core laptops, that each core has 2 GB of ram to attain the convergence criteria of 10^{-4} . As a result, the highest enhancement through the simulation, is achieved when b and a are 20 and 55, respectively, and CP development also occurred when α is between (55 and 60) and β is 55. impact of the DGV is a bit higher in lower TSR, and maximum improvements are 16.9%, 38.8%, 42.2%, 27.4% and 27.7 for TSR 3, 4, 5, 6 and 7 respectively, while a and b are 55 and 20. Briefly, based on previous Figs, maximum output of the VAWT are captured when DGV is in optimum position ($\beta = 20$ and $\alpha = 55$). Hence, comparison of the CP with and without DGV in four considered TSRs, investigated in this study and illustrated in Fig. 8. As can be seen in Fig. 8, maximum CP of the open and augmented rotor are 0.47 and 0.55, respectively, in $TSR = 5.901$.

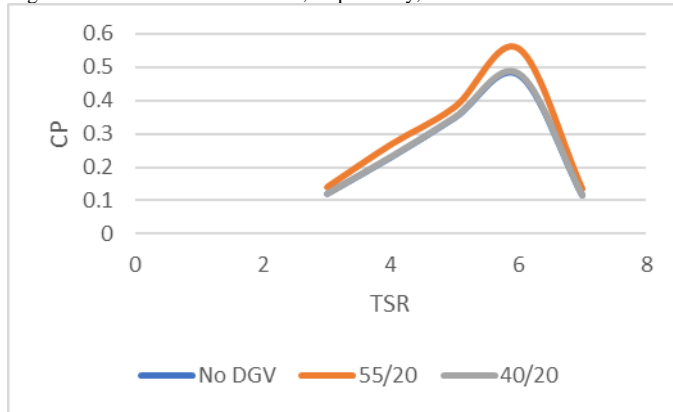


Fig. 8. Comparison of the CP with and without DGV in five tested TSR

In all range of the TSRs, the simulated results also showed that DGV can improve the CP more than 35% when $\beta = 20$ and $\alpha = 55$. Significant improvement in C_m is achieved when $\beta = 20$ and $\alpha = 55$ within $\theta = 137$ – 182 , however negative effect in C_m made after $\theta = 200$. Furthermore, C_m variations based on the different azimuth θ and DGV (β and α) angles, in one rotation and constant TSR are shown in Fig. 9.

Fig. 9 shows that significant improvement in terms of the magnitude of the velocity and angle of the inlet velocity is achieved when the azimuth angle is zero. Therefore, compared with the open rotor, C_m starts to reach the higher position in three different angles of the augmented rotor, when $\theta = 0$. Farther, negative impact of the ODGV can be seen in these different three cases, when azimuth angle is between 100 and 136. Application of the DGV with ($\beta = 20$ and $\alpha = 40$) and ($\beta = 20$ and $\alpha = 55$) also helps to improve the torque generation in VAWT, when azimuth angle is between 136 and 180. Whilst DGV with ($\beta = 20$ and $\alpha = 40$) has negative effect on lower azimuth angles. In conclusion, the DGV with ($\beta = 20$ and $\alpha = 55$), is the best option to improve the torque generation in VAWT. These results can also be validated by velocity vectors explained in the following section.

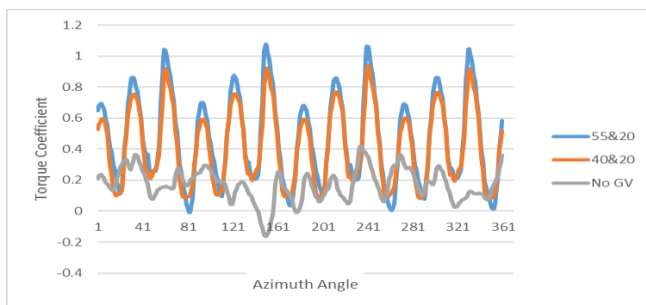


Fig. 9. Torque coefficient (C_m) variation in one rotation with different DGV

4.2 Velocity contours

The inlet velocity to the VAWT is usually enhanced to higher amount, so the velocity of the wind streamlines can be investigated to compare fluids around VAWT with and without augmented DGV cover. Fig. 10 shows the simulation of streamlines around the VAWT and DGV guide vane. Based on Fig. 10, inlet velocity angle and magnitude have been considerably enhanced by means of the DGV cover in the optimal DGV position. Further, velocity vectors in two different locations of the VAWT blades ($\theta = 0$ and $\theta = 120$) where three different positions compared with open rotor in each location, are presented in Figs. 11 and 12. According to Fig. 11, the inlet velocity has been improved by using DGV cover in all three mentioned range of b and a . Comparison between Fig. 12 (part B and D) and Fig. 9 shows that DGV had positive effects on the velocity, and the outputs of the torque have been enhanced via DGV. In addition, the main point of these types of Figs can be seen in Fig. 12 (part C), where the negative influence of the DGV is the most in comparison with other positions. Indeed, the role of DGV is like a barrier for the inlet velocity and has negative impact on the torque.

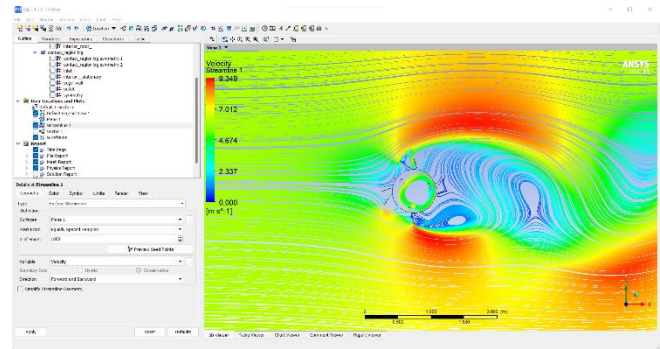


Fig. 10. Streamlines on VAWT and DGV $b = 20$ and $a = 55$ in $TSR = 3$.

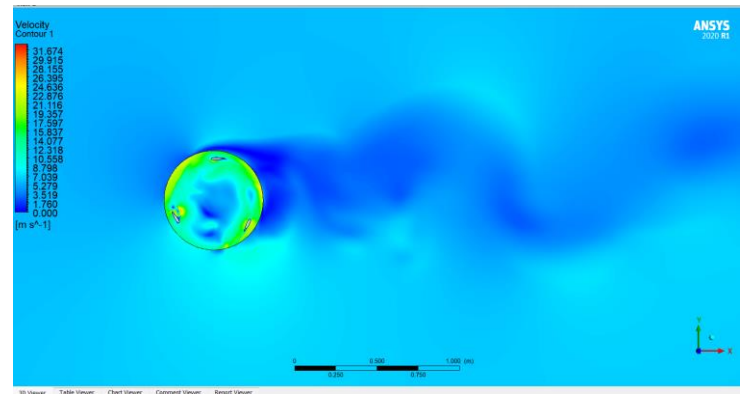


Fig. 11. A

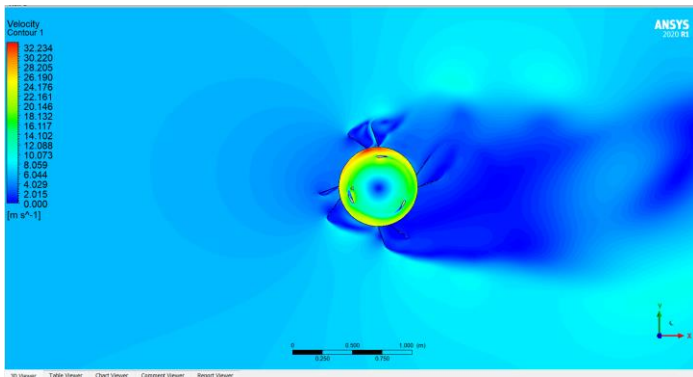


Fig. 11. B

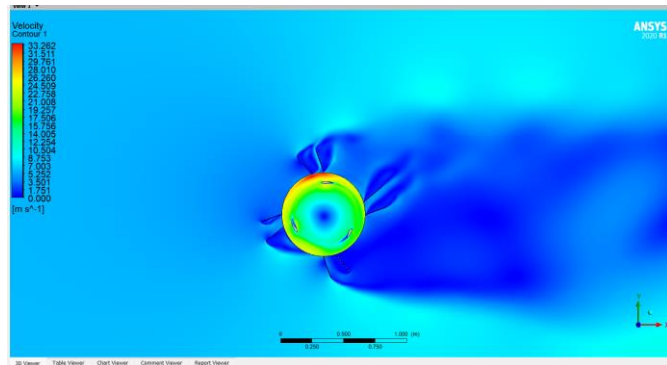


Fig. 11.C

Fig. 11. Velocity contours when $\theta = 0$ for three position including A (open rotor), B ($\beta = 20$ and $\alpha = 55$), C ($\beta = 20$ and $\alpha = 40$).

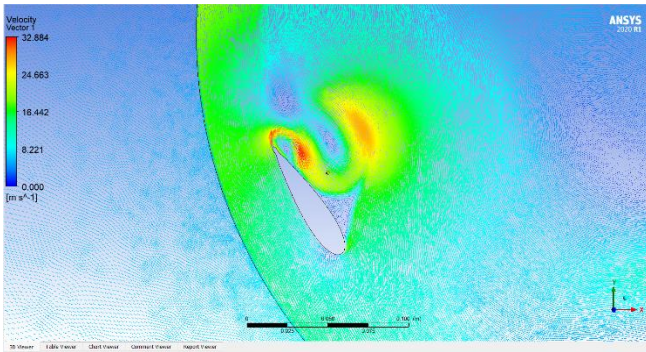


Fig. 12. Vectors when $\theta = 120$ for (open rotor)

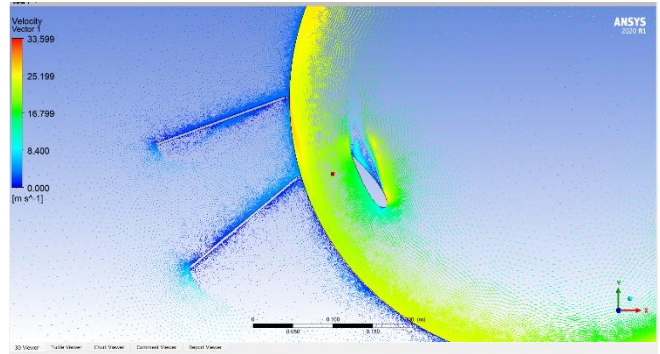


Fig. 13. Vectors when $\theta = 120$ for A ($\beta = 20$ and $\alpha = 55$)

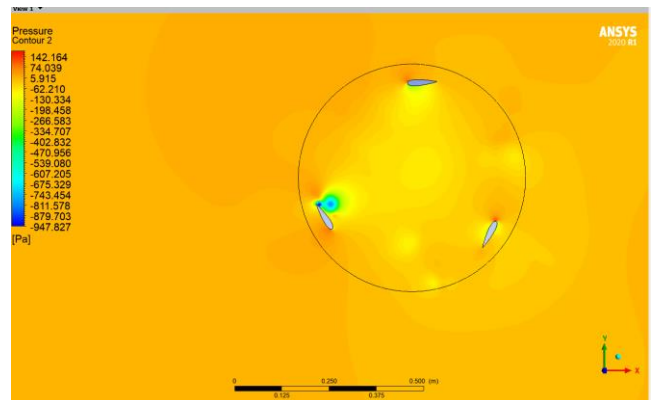


Fig. 14. Pressure contour for open rotor

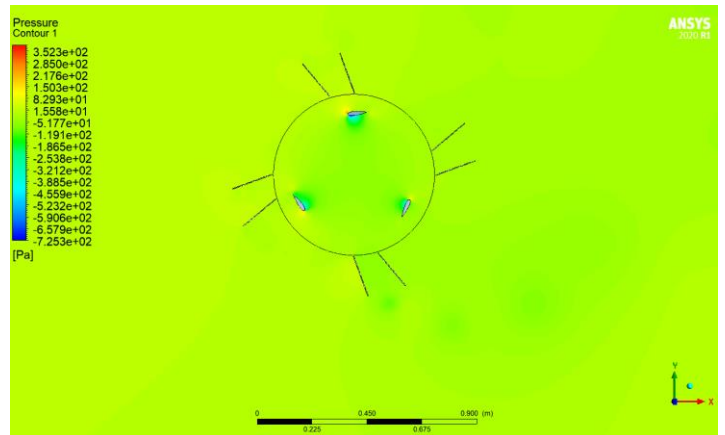


Fig. 15. Pressure contour for A ($\beta = 20$ and $\alpha = 55$)

5.CONCLUSION

In this study, numerical and experimental simulations were conducted on a Darrius-type VAWT which has been shrouded by DGV cover. The main goal of this study is to obtain the best position of the guide vane angles to achieve the maximum performance of the VAWT. For this purpose, grid dependency study was designed to determine the best and high-quality mesh. Effects of the Domain size were also investigated, and the results showed that domain with the size of a 12D height (side walls distance) and 30D for domain length has no effect on CP prediction of VAWT. Furthermore, outputs of the simulation were compared with experimental data and results showed that good agreement is achieved in two-dimensional simulation. The effects of the DGV angles on the performance of the VAWT were investigated in this study and the results have been proposed in Fig (Figs.9). Additionally, two different arrangements of the first and second angles of the DGV (β and α) were considered in five different TSRs, to obtain the best numerical simulation. In conclusion, the best simulation results were obtained for DGV with ($\beta = 20$ and $\alpha = 55$), which increased the CP of the VAWT by 16.9%, 38.8%, 42.2%, 27.4% and 27.7% when TSR is 3, 4, 5, 6 and 7, respectively

ACKNOWLEDGMENT

LAST BUT NOT LEAST, I WOULD LIKE TO THANK EVERYONE WHO HELPED ME IN THIS VERY SIMPLE WORK, THEY ARE DR. RADWA ABED GHAZALA, WHO IS MY SUPERVISOR IN THIS RESEARCH, AND FROM HER EXPERIENCE IN THE FIELD OF WIND TURBINES, I LEARNED FROM HER EVERYTHING I KNOW ABOUT WIND TURBINES, AND ALSO I WOULD LIKE TO THANK THE HIGHER INSTITUTE OF TECHNOLOGY IN THE TENTH OF RAMADAN, BECAUSE THIS EDUCATIONAL PLACE HELPED ME A LOT AND MADE THINGS SIMPLER IN THIS RESEARCH. I ALSO THANK ALL MY COLLEAGUES AT THE INSTITUTE BECAUSE THEY REALLY HELPED ME IN THIS WORK.

REFERENCES

- [1] Howell, Robert, Ning Qin, Jonathan Edwards, and Naveed Durrani. "Wind tunnel and numerical study of a small vertical axis wind turbine." *Renewable Energy* 35 (2010): 412-422.
- [2] Beri, H., and Y. Yao. "Effect of Camber Airfoil on Self-starting of Vertical Axis Wind Turbine." *Journal of Environmental Science and Technology* 4-3 (2011): 302-312.
- [3] Raciti Castelli M, Englaro A, Benini E. The Darrieus wind turbine: proposal for a new performance prediction model based on CFD. *Energy* 2011; 36:4919-34
- [4] Wakui, Tetsuya, Yoshiaki Tanzawa, Takumi Hashizume, and Toshio Nagao. "Hybrid Configuration of Darrieus and Savonius Rotors for Stand-Alone Wind Turbine- Generator systems. *Electr Eng Jpn* 2005; 150(4):13-22.
- [5] Chong W, Fazlizan A, Poh S, Pan K, Hew W, Hsiao F. The design, simulation, and testing of an urban vertical axis wind turbine with the Omni-direction-guidevane. *Appl Energy* 2013; 112:601–9.
- [6] Nobile R, Vahdati M, Barlow JF, Mewburn-Crook A. Unsteady flow simulation of a vertical axis augmented wind turbine: a two-dimensional study. *J Wind Eng Ind Aerodyn* 2014; 125:168–79.
- [7] Malki R, Williams A, Croft T, Togneri M, Masters I. A coupled blade element momentum computational fluid dynamics model for evaluating tidal stream turbine performance. *Appl Math Model* 2013;37(5):3006–20.
- [8] Li Y, Calisal SM. Three-dimensional effects and arm effects on modeling a vertical axis tidal current turbine. *Renew Energy* 2010;35(10):2325–34.
- [9] Wekesa DW, Wang C, Wei Y, Danao LAM. Influence of operating conditions on unsteady wind performance of vertical axis wind turbines